Title:

SUMOylation of rice DELLA SLR1 modulates transcriptional responses and improves yield under salt stress

Authors:

Nuno M. Gonçalves[a*], Telma Fernandes[a], Cátia Nunes[b**], Margarida T. G. Rosa[a], Cleverson C. Matiolli[a], Mafalda A. A. Rodrigues[a], Pedro M. Barros[a], M. Margarida Oliveira[a], Isabel A. Abreu[a1]

Affiliations:

[a] Instituto de Tecnologia Química e Biológica, Universidade Nova de Lisboa (ITQB NOVA), 2780-157, Oeiras, Portugal

[b] Instituto de Biologia Experimental Tecnológica (iBET), 2780-157, Oeiras, Portugal

Author Contributions:

NMG participated in the conception of research, executed most experiments, and wrote the article with contributions from all authors. TF did protein interaction experiments. MTGR characterized SUMO-protease rice lines. CCM analysed data and completed the writing. MAAR purified recombinant proteins. PMB analysed RNA seq. MMO supervised experiments and analysed results. IAA conceived original project, supervised experiments, and finalized the article.

Contact:

[1] Corresponding Author:

Isabel A. Abreu

Instituto de Tecnologia Química e Biológica, Universidade Nova de Lisboa (ITQB NOVA), 2780-157, Oeiras, Portugal, Tel.: +351 214469647, E-mail: abreu@itqb.unl.pt

***** Currently at Leibniz Institute of Plant Biochemistry (IPB), Weinberg 3 | 06120 Halle | Germany (nunomiguel.goncalves@ipb-halle.de)

** Currently at Instituto Nacional de Investigação Agrária e Veterinária, Avenida da República, Oeiras, Portugal (catia.soares@iniav.pt)

Short title (50 characters): SUMOylation of rice SLR1 increases salt tolerance

ABSTRACT

DELLA proteins modulate GA signalling and are major regulators of plant plasticity to endure stress. DELLAs are mostly regulated at the post-translational level, and their activity relies on the interaction with upstream regulators and transcription factors (TFs). SUMOylation is a post-translational modification (PTM) capable of changing protein interaction and found to influence DELLA activity in Arabidopsis. We determined that SUMOylation of the single rice DELLA SLENDER RICE1 (SLR1) occurs in a lysine residue different from the one previously identified in Arabidopsis REPRESSOR OF GA (RGA). Remarkably, artificially increasing SUMOylated SLR1 (SUMO1SLR1) levels attenuated the penalty of salt stress on plant yield. Gene expression analysis revealed that the overexpression of SUMOylated SLR1 regulates key dioxygenases that modulate active GA levels, namely *GA20ox2* and *GA2ox3*, which could partially explain the sustained productivity upon salt stress imposition. Besides, SLR1 SUMOylation blocked the interaction with the growth regulator YAB4, which may fine-tune *GA20ox2* expression. Mechanistically, we propose that SLR1 SUMOylation disrupts the interaction with members of several transcription factor families to modulate gene expression. We found that SLR1 SUMOylation represents a novel mechanism modulating DELLA activity, which attenuates the impact of stress on plant performance.

Keywords: DELLA, SUMOylation, stress, productivity, SLR1, YAB4, bZIP23, gibberellin

One sentence summary: Rice plants show increased yield under salt stress when its gibberellin transcriptional regulator DELLA protein is artificially SUMOylated.

INTRODUCTION

Salinity is one of the most serious threats to food security, affecting 20% of irrigated soils worldwide. Rice (*Oryza sativa* L.) is a crop with high sensitivity to salinity compared to other monocot crops, such as wheat and barley (Munns and Tester, 2008). Plant sessile nature requires rapid physiological responses to cope with stress, which is partly achieved through a complex crosstalk between hormone signalling pathways affecting growth, flowering, and defence against environmental challenges (Vanstraelen and Benková, 2012). Gibberellins (GA) are diterpenoid hormones involved in the regulation of several developmental processes, including seed germination, stem elongation, and flowering (Hirano et al., 2008). GA responses are modulated by DELLA proteins, which act as transcriptional regulators (Hedden and Thomas, 2012). In the presence of GA, DELLAs are targeted to ubiquitin-mediated proteasome degradation by the GA-receptor GA-INSENSITIVE DWARF1 (GID1) through binding to specific DELLA domains (DELLA/TVHYNP), followed by DELLA polyubiquitination mediated by the E3-ligase GA-INSENSITIVE DWARF2/SLEEPY1 (GID2/SLY1). When GA levels decrease, DELLA proteins accumulate and interact with key transcriptional regulators to restrain growth (Hirano et al., 2010; 2008; Ueguchi-Tanaka et al., 2008). For instance, DELLAs can sequester the transcription factors PHYTOCHROME INTERACTING FACTOR3 and 4 (PIF3 and PIF4), in addition to negatively regulate PIF3 protein abundance, mediating the crosstalk of light and GA signalling to modulate cell growth (de Lucas et al., 2008; Li et al., 2016). DELLA transcriptional regulation of GA biosynthetic genes responsible for hormonal homeostasis also potentiates growth arrest. The single rice DELLA SLENDER RICE1 (SLR1) interacts with YAB4 transcription factor to prevent the induction of *GA20ox2*, which encodes a dioxygenase that is essential for the synthesis of bioactive GA (Yang et al., 2016). In Arabidopsis, DELLA interaction with GAI-ASSOCIATED FACTOR1 (GAF1) TF triggers a negative-feedback loop that activates GA biosynthesis and subsequent DELLA degradation (Fukazawa et al., 2017). The increasing number of validated DELLA interactors showcase an overlap with most hormone pathways, impacting development, fertility, and seed number (Davière and Achard, 2015; Van De Velde et al., 2017).

DELLA activity is mostly modulated through post-translational modifications (PTMs), which impact its ability to interact with transcriptional regulators and modulate gene expression (Van De Velde et al., 2017). Besides ubiquitination and subsequent

94 proteasome-mediated degradation, there are other PTMs that influence the activity of
95 the DELLA's in response to GA signalling. For instance, the phosphorylation by kinase
96 EARLY FLOWERING 1 (EL1) regulates SLR1 protein stability and activity (Dai and
97 Xue, 2010; Itoh et al., 2005). Recently, a mechanism of antagonistic PTMs was
98 proposed to regulate Arabidopsis DELLA's interaction with specific protein partners.
99 *O*-fucosylation by SPINDLY (SPY) promotes DELLA interaction with essential growth
100 regulators – such as BRASSINOLE-RESISTANT1 (BZR1), PIF3 and PIF4 – leading
101 to growth arrest (Zentella et al., 2017). Conversely, RGA *O*-GlcNAcylation by SECRET
102 AGENT (SEC) blocks these interactions and promotes GA-induced growth resumption
103 (Camut et al., 2017; Zentella et al., 2016). DELLA SUMOylation has also been
104 indicated as a PTM controlling the stability of REPRESSOR OF GA (RGA), one of the
105 Arabidopsis five DELLA proteins. SUMO attachment to RGA hinders its ubiquitin-
106 mediated proteasome degradation through blockage of GID1-RGA interaction in a GA-
107 independent manner (Conti et al., 2014). The stabilization of Arabidopsis DELLA by
108 SUMOylation also positively affected salt stress response, in line with observations
109 that DELLA accumulation leads to increased salinity tolerance (Achard et al., 2006;
110 Conti et al., 2014; Nelis et al., 2015). SUMOylation is a eukaryotic ubiquitination-like
111 process that involves the processing, activation, conjugation, and ligation of mature
112 SMALL UBIQUITIN-LIKE MODIFIER (SUMO) to acceptor lysine's (K) in the target
113 protein (Miura et al., 2007). Unlike ubiquitination, SUMO-modifications often occur in
114 a canonical consensus motif (ψ-K-X-E/D), which can be used for *in silico* prediction of
115 SUMOylation targets (Xue et al., 2006). SUMOylation regulates protein stability,
116 activity, and interactions with specific protein partners (Cremona et al., 2012). SUMO
117 deconjugation (deSUMOylation) from target proteins is performed by deSUMOylating
118 proteases (DSPs), with some members recently reported to be specific for poly-SUMO
119 chain processing (Eckhoff and Dohmen, 2015; Yates et al., 2016; Augustine et al.,
120 2018). In rice, reduced levels of SUMO conjugates due to DSP activity of
121 OVERTOLERANT TO SALT1/2 (OTS1/OTS2) have been connected to increased salt
122 tolerance (Srivastava et al., 2016a; 2016b). SUMOylation of specific TFs, such as the
123 stress-induced basic LEUCINE ZIPPER 23 (bZIP23), was suggested to be crucial to
124 drought tolerance and fertility (Srivastava et al., 2017).
125 Few studies have addressed the biological function of SUMOylation of stress-
126 induced targets. Moreover, most of the studies investigating the effects of PTMs on

127 DELLA function were done in Arabidopsis. This dicot model plant encodes five
128 DELLAs in the genome and essentially differs from monocots, which harbour a single
129 DELLA gene. This study demonstrates that SUMOylation of the single rice DELLA
130 SLR1 impacts the transcriptional output in response to salt stress, possibly through
131 modulation of SLR1 interaction with transcription factors regulating transcriptional
132 patterns governing plant growth and stress responses. We suggest that SLR1
133 SUMOylation affects its interaction with key transcription factors that impacts GA
134 homeostasis (YAB4), ABA signalling (bZIP23), and JA signalling (bHLH089/94).
135 Additionally, the evidence provided suggests that it is possible to uncouple stress
136 response from decreased plant performance by manipulating the levels of
137 SUMOylated SLR1.
138
139 **RESULTS**
140 **SLR1 SUMOylation *in vitro* analysis suggests diversification of DELLA**
141 **regulation by SUMO in plants**
142 SUMOylation of lysine 65 (K65) in Arabidopsis DELLA RGA modulates its
143 stability in a GA-independent manner (Conti et al., 2014). To determine rice SLR1
144 SUMOylation, we started by performing an *in silico* prediction of SUMOylation motifs
145 using SUMOsp2 software (Xue et al., 2006) in rice DELLA SLR1 and Arabidopsis
146 DELLA RGA protein sequences. We sought for putative conserved SUMOylation
147 motifs in both proteins and found a low probability SUMOylation site which
148 corresponds to Arabidopsis RGA (Figure 1A). The SUMO acceptor lysine (K65) in
149 RGA is part of a canonical SUMOylation motif (LKLE). In contrast, its counterpart in
150 SLR1(K60) is not part of a canonical motif (QKLE), nor are the equivalent ones in
151 another Arabidopsis or monocot DELLAs (Supplemental Figure S1). Nevertheless,
152 both SLR1 and RGA have a high probability SUMOylation site on lysine 2 (K2).
153 To verify if the *in silico* prediction of SUMO attachment to SLR1 holds true, we
154 performed an *in vitro* SUMOylation assay targeting both full-length SLR1 and a
155 truncated isoform containing the leading 190 amino acids (SLR1t). Importantly, SLR1t
156 includes the N-terminal domains (DELLA and TVHYNP) responsible for GA-mediated
157 modulation of DELLA stability and SLR1 transactivation properties (Davière and
158 Achard, 2015; Marín-de la Rosa et al., 2015; Hirano et al., 2012), as well as the
159 predicted SUMOylation sites depicted in the Figure 1A. We observed a mobility-shift
160 of both full-length SLR1 (Figure 1B) and truncated SLR1t (Figure 1C; with both

161 SUMO1 and SUMO2 - Supplemental Figure S2A-B), consistent with ATP-dependent
162 SUMO-conjugation in the presence of the rice SUMOylation machinery. The band
163 resulting from *in vitro* SLR1 and SLR1t SUMOylation disappeared upon treatment with
164 recombinant SUMO-specific protease ULP1 that cleaves SUMO from its conjugates
165 (Li and Hochstrasser, 2003), confirming that the observed mobility-shift was caused
166 by attached SUMO (Figure 1B-C). To analyse the contribution of each predicted
167 SUMO acceptor lysine in SLR1, we performed directed mutagenesis changing the
168 lysines K2 and K60 to arginine residues, which cannot be conjugated to SUMO (K2R
169 and K60R). The mutated SLR1t K60R isoform retained the ability to be SUMOylated
170 – which was confirmed by the band disappearance after SUMO proteolytic removal by
171 ULP1 treatment – while K2R did not (Figure 1C). The result shows that K2 is the
172 preferential SUMOylated residue in SLR1, suggesting that SUMO attachment to
173 DELLA may occurs in distinct lysine residues of Arabidopsis RGA (K65) and rice SLR1
174 (K2). SUMOylation in different sites potentially results in different outcomes regarding
175 protein interactions and activity of SUMOylated SLR1 compared to SUMOylated RGA.
176 However, the *in silico* prediction of SUMOylation sites suggests that RGA K2 could
177 also be SUMOylated (Figure 1A). We need further studies to clarify if K2 SUMOylation
178 occurs in Arabidopsis RGA, or even in DELLA proteins from other species.
179
180 **SUMO protease activity analyses provide evidence of *in vivo* SLR1 SUMOylation**
181 To demonstrate the *in vivo* SUMOylation of SLR1, we treated non-denatured
182 rice protein extracts with the ULP1 SUMO protease. The procedure would allow for
183 indirect detection of SUMOylated SLR1 by analysing the increase in non-SUMOylated
184 SLR1 protein amount resulting from ULP1 treatment, in comparison to SUMOylated
185 SLR1. We observed an increase of non-SUMOylated SLR1 upon the addition of ULP1,
186 as detected by the anti-SLR1 antibody in protein extracts (Figure 2A). The result is in
187 line with the previous *in silico* and *in vitro* analyses indicating that SLR1 could be
188 SUMOylated. Our results also suggest that SLR1 mono-SUMOylation may be much
189 less abundant than other forms of SUMOylation since we could not detect an SLR1
190 band with the expected mobility shift for mono-SUMOylation (Figure 1B-C). To further
191 support the evidence of *in vivo* SLR1 SUMOylation, we tested the levels of
192 SUMOylated SLR1 in knockout mutant lines for genes encoding rice SUMO
193 proteases, namely *els1* and *fug1* (Figure 2B-C). ELS1 and FUG1 are active rice SUMO
194 proteases, as both knockout lines contain increased levels of SUMOylated proteins

195 (Rosa et al., 2018). We treated protein extracts from *els1* and *fug1* homozygous lines
196 with ULP1 and compared their total SUMOylated SLR1 levels with those present in
197 negative segregant lines (NS). The results show that although the overall level of non-
198 SUMOylated SLR1 is not significantly affected in either one of the KO lines when
199 compared to their negative segregant lines (Figure 2B), the levels of SUMOylated
200 SLR1 are increased in *fug1* mutant (Figure 2C). These results demonstrate
201 SUMOylation of SLR1 occurs *in vivo*, as indicated by the processing (*i.e.,* switch from
202 SUMO-SLR1 to SLR1) mediated by FUG1. Interestingly, it also suggests that there is
203 a certain degree of specificity for SLR1 deSUMOylation, as suggested by SUMO
204 cleavage by FUG1 and not ELS1 (Figure 2C). Altogether, the evidence supports that
205 SLR1 is SUMOylated *in planta* and that SUMO specific proteases could regulate the
206 levels of SUMOylated SLR1.
207
208 **Overexpression of SUMOylated SLR1 increases salt tolerance**
209 Because DELLA protein accumulation was previously connected with stress
210 tolerance (Achard et al., 2006), we assessed SLR1 expression in response to salt
211 stress. Wild-type seedlings accumulated SLR1 protein in shoots during the first 8
212 hours of stress (Supplemental Figure S3A). On the other hand, *SLR1* transcript levels
213 decreased, which is consistent with the previously reported DELLA negative feedback-
214 loop regulation on its own transcript abundance (Hedden & Thomas, 2012).
215 To gain insight on the role of SLR1 SUMOylation in rice development and
216 responses to salt stress, we generated transgenic lines overexpressing SLR1 (SLR1-
217 OX), as well as lines constitutively expressing a mimicry of the SUMOylated form of
218 SRL1 (SUMO1SLR1-OX) originated from the genetic fusion of mature SUMO1 to the
219 K2 residue, which is the SUMOylated lysine of SLR1 ($SUMO1_{GG}$::$SLR1_{K2}$) (Figure 3A).
220 The strategy of using SUMOylated mimetic isoforms originated by gene fusion with
221 the SUMO coding sequence has been used in several biological systems, including
222 plants (Crozet et al., 2015; Ulrich, 2008). We confirmed the overexpression of non-
223 SUMOylated SLR1 isoforms in both SLR1-OX and SUMO1SLR1, with the latter also
224 showing a band with the expected mobility-shift of SLR1 corresponding to mono-
225 SUMOylation (Figure 3B). We also observed an increase in the amount of non-
226 SUMOylated SLR1 protein in SUMO1SLR1-OX compared to WT and NS lines, which
227 could be arising from the processing by endogenous SUMO proteases because the
228 fusion protein retains the SUMO diglycine protease cleavage motif (-GGK-).

229 Rice is particularly sensitive to salt at both seedling and booting stages
230 (Gregorio et al., 1997). Therefore, we analysed stress marker symptoms of SLR1-OX
231 and SUMO1SLR1-OX lines subjected to high salt concentrations at seedling stage, as
232 well as yield parameters on salt treatments at booting stage. Evaluation of symptoms
233 in seedlings subjected to severe salinity (120mM NaCl) for 8 days showed that both
234 SUMO1SLR1-OX lines performed better under salt stress, displaying decreased
235 symptoms severity according to SES score (Standard Evaluation System for Rice) by
236 IRRI (International Rice Research Institute) (Gregorio et al., 1997), including minimal
237 leaf tip rolling and increased survival (Figure 3C). Importantly, salt tolerance could be
238 correlated with SUMOylated SLR1 levels, as SUMO1SLR1-OX #1 – showing higher
239 SLR1 SUMOylation levels compared to SUMO1SLR1-OX #2 – performed better than
240 the latter (Figure 3B-C). Interestingly, salt-induced SUMOylated SLR1 increased
241 alongside with the non-SUMOylated SLR1 in SUMO1SLR1-OX lines (Supplemental
242 Figure S3B), suggesting that SUMO cleavage processing could be occurring
243 alongside the duration of salt stress. Plants overexpressing SUMO1SLR1 and SLR1-
244 OX also recovered better than the wild type Nipponbare in the 8 following days to salt
245 stress cessation. Thus, mild overexpression of SLR1 can increase rice tolerance to
246 salinity, and this effect is increased by its SUMOylation.
247 We next tested rice performance under salt stress at the booting stage. Panicle
248 initiation was the cue for mild salt stress imposition (80 mM NaCl), as at this
249 developmental stage pollen viability is most affected by high salinity (Negrão et al.,
250 2011; Sarhadi et al., 2012). Upon measurement of agronomical parameters, we did
251 not detect stress-induced changes in plant height (Figure 4A), tillering or panicle length
252 (Supplemental Figure S4) when compared to the control. However, two critically
253 important parameters for rice yield – namely fertility (filled grains) and productivity
254 (grain weight) – were significantly improved in SUMO1SLR1-OX lines under mild salt
255 stress. Both SLR1-OX and Nipponbare presented around 10% decrease in fertility
256 when comparing to mock conditions, while SUMO1SLR1-OX showed the same fertility
257 in both salt and mock treatments (Figure 4B). This tendency was also observed in
258 grain weight, where SUMO1SLR1-OX presented higher tolerance to mild salt stress
259 regarding productivity compared to Nipponbare and SLR1-OX (Figure 4C). Although
260 the SUMO1SLR1-OX lines had lower productivity under mock conditions compared to
261 Nipponbare, they showed improved performance under salt stress. These results

262 substantiate the significance of SUMOylation of SLR1 in salt stress tolerance
263 acquisition and yield protection observed in two sensitive rice developmental stages.
264
265 **SLR1 SUMOylation regulates GA biosynthetic pathway transcripts in response**
266 **to salt stress**
267 The salt tolerance observed in SUMO1SLR1-OX lines could not be attributed
268 to the increased accumulation of SLR1, as SLR1 protein levels were similar in the
269 SLR1-OX and SUMO1SLR1-OX transgenic lines (Figure 3B). Thus, we inferred that
270 the observed phenotypes in SUMO1SLR1-OX lines could be a consequence of the
271 increased levels of SUMOylated SLR1. Because DELLA proteins regulate
272 transcription, we performed a genome-wide expression analysis to identify
273 differentially regulated genes in SLR1-OX and SUMO1SLR1-OX that could explain
274 the phenotypical differences observed in these lines in response to salt stress. We
275 exposed SLR1-OX, SUMO1SLR1-OX, and Nipponbare genetic background to high
276 salt concentrations (120 mM NaCl) during 8 hours at the seedling stage (2 weeks old),
277 and collected samples for subsequent RNA-seq analysis (Supplemental Table S1).
278 We selected the lines SLR1-OX #2 and SUMO1SLR1-OX #2 for the RNA-seq assay
279 because they showed similar non-SUMOylated SLR1 levels, as we aimed to tackle
280 the effect of SLR1 SUMOylation on gene expression. Both overexpressor lines
281 showed an approximately 1.8-fold increase in SLR1 transcript levels when compared
282 to Nipponbare, which is in line with the levels validated by real-time qPCR for the same
283 samples, *ca.* 1.5-fold increase (Supplemental Figure S5), and with protein levels
284 assessed by immunoblotting (Figure 3B). The induction of salt-induced genes *Rab21*
285 and *P5CS* was used as a transcriptional readout of the salt stress treatment efficiency
286 (Supplemental Figure S5).
287 Principal Component Analysis (PCA) revealed a clear separation of samples by
288 treatment, this factor being responsible for 47% of the variability in gene expression,
289 while genotype-specific transcriptomic changes explained 21% of the observed
290 variability (Supplemental Figure S6). The constitutive overexpression of SLR1 and
291 SUMO1SLR1 in absence of salt stress resulted in differential regulation of 247 and
292 207 genes, respectively (Supplemental Tables S1.6 to S1.8). Functional annotation of
293 SLR1-OX DEGs showed enrichment of gene ontology (GO) terms associated with
294 diterpenoid biosynthesis, highlighting the impact of SLR1 on GA metabolism
295 (Supplemental Figure 7A and Supplemental Tables S1.6 to S1.7). Notably, we

296 observed overall downregulation in genes coding for enzymes essential in non-
297 gibberellin diterpenoid synthesis, namely syn-copalyl diphosphate synthase (*CPS4*)
298 and ent-cassa-12,15-diene synthase (*KSL7*) (Supplemental Figures S7A and S7C).
299 These enzymes are part of a diterpenoid pathway branching point that feeds the
300 phytoalexins biosynthetic pathway (Otomo et al., 2004). Concurrently, other genes
301 related to phytoalexin and phytocassane synthesis, such as cytochrome P450 family
302 members *CYP701A8/KO1, CYP99A3, CYP71Z6, CYP76M8,* and *CYP71Z7*, were
303 also downregulated in SLR1-OX.
304 Phenotypical discrimination of SLR1-OX and SUMO1SLR1-OX was observed
305 under salt stress but not under control conditions (Figure 3C). Interestingly, a closer
306 look into the distribution of SLR1-OX and SUMO1SLR1-OX samples in the PCA, under
307 control and stress conditions highlights a similar tendency (Supplemental Figure S6).
308 Hence, we focused on the analysis on the 236 DEGs specific to SUMO1SLR1-OX
309 exposed to salt stress. After functional annotation of DEGs specific to SUMO1SLR1-
310 OX, we found a significant over-representation of GO terms associated with defence
311 response and gibberellin dioxygenase activity (Supplemental Figures S7B and S7C).
312 We also found a salt stress-dependent induction of *GA20ox2* and *GA2ox3* genes in
313 SUMO1SLR1-OX (Supplemental Table S1.4). *GA20ox2* and *GA2ox3* encode
314 enzymes involved in the regulation of active GA (GA_4) levels. Therefore, it is
315 reasonable to hypothesize that SLR1 SUMOylation could adjust active GA
316 homeostasis upon exposure to salt stress (Supplemental Figure S7C).
317
318 **SUMOylation disrupts SLR1 interaction with stress-associated transcription**
319 **factors**
320 The increased salt tolerance and sustained productivity of SUMO1SLR1-OX
321 under salt stress likely arise from the presence of increased levels of SUMOylated
322 SLR1 (Figure 3B-C; Figure 4A-B), which seems to be affecting the gene expression
323 profile of plants exposed to stress. The *GA20ox2* transcript was induced around 2-fold
324 in SUMO1SLR1-OX exposed to salt stress, while it showed only a marginal induction
325 in SLR1-OX under the same conditions (Supplemental Table S1.2). One possible
326 mechanism by which SLR1 could affect *GA20ox2* transcription is through the
327 interaction with the transcription factor YAB4, thereby repressing the expression of
328 *GA20ox2* (Yang et al., 2016). We did not detect *YAB4* transcript changes after 8 hours
329 of salt stress exposure, but a search in public transcriptome data revealed that *YAB4*

330 is induced in rice shoots after 3h of salt stress imposition (Genevestigator - Hruz et al.,
331 2008; Supplemental Figure S9A-B), which could lead to increased YAB4 protein
332 accumulation during later stages of plant adaptation to salt stress. In an attempt to
333 dissect the molecular pathways involved in *GA20ox2* upregulation in SUMO1SLR1-
334 OX, we verified the interaction of SLR1 and SUMOylated SLR1 with YAB4 TF using a
335 yeast two-hybrid system and bimolecular fluorescence complementation (BiFC). The
336 aim was to test the effect of SUMOylation on SLR1-YAB4 interaction, which could
337 affect *GA20ox2* transcription. We used a variant of the SUMO1SLR1 fusion protein
338 lacking the SUMO protease recognition domain to avoid possible processing by yeast
339 SUMO proteases (SUMO1($_{GG-AA}$)::SLR1). We confirmed the previously demonstrated
340 interaction between SLR1 and YAB4 (Yang et al., 2016), and also found that the
341 mimicking SUMOylation in lysine 2 of SLR1 disrupts SLR1-YAB4 interaction in both
342 yeast and *in planta* (Figure 5A-B; negative controls in Supplementary Figure S8). The
343 blocking of the SLR1 interaction with YAB4 by SUMO correlates with the induction of
344 *GA20ox2* in salt-stressed SUMO1SLR1-OX lines.

345 To further evaluate the molecular aspects of SUMO1SLR1-OX tolerance to salt
346 stress, we explored the notion that SLR1 exerts its function mainly by transcriptional
347 regulation through interaction with transcription factors. We designed a strategy that
348 allowed us to identify SLR1 TF interactors that could explain, at least partially, the
349 differences in gene expression observed in the transgenic lines upon exposure to salt
350 stress. Briefly, we submitted the promoter sequences (1000 bp upstream to the
351 Transcription Start Site – TSS) of 417 selected DEGs (SLR1- and SUMO1SLR1-
352 dependent salt stress responsive genes; Supplemental Tables S1.3 and S1.4) to an
353 *in silico* search for transcription factor binding sites (TFBS) in the PlantPAN online
354 database (Chow et al., 2016). Next, we selected only TFBS and corresponding binding
355 TFs that have been experimentally validated. This allowed us to identify TFs from the
356 TCP, bZIP, bHLH, and B3 families that could be regulating the output gene expression
357 of SLR1-OX and SUMO1SLR1-OX transgenic lines under salt stress (Table 1). To
358 cross-validate the TF identification, we made sure that a substantial overlap between
359 the known target genes of those TFs and the SLR1- and SUMO1SLR1-dependent
360 DEGs were observed (Supplemental Tables S1 and S2).

361 The interaction between SLR1 with the selected candidates (Table 1) and its
362 regulation by SUMOylation was assessed through Y2H assays and BiFC analyses
363 (Figure 5A-B). The basic helix-loop-helix transcription factors bHLH089 and bHLH094,

364 as well as the homeobox TF OSH1, showed a strong interaction with SLR1 but not
365 with SUMO1($_{GG-AA}$)::SLR1. This finding suggests that SUMOylation could modulate
366 the binding of SLR1 to these transcription factors, potentially affecting their
367 transcriptional activities. We also found that bZIP23 can interact with both
368 SUMOylated and non-SUMOylated SLR1 (Figure 5A). The interaction of SLR1 with
369 bHLH089 and bHLH094, as well as its disruption by SLR1 SUMOylation, was validated
370 through BiFC in *Nicotiana benthamiana* leaves, supporting the *in planta* SUMO-
371 dependent regulation of these interactions (Figure 5B). Neither IDEF1 nor PCF1
372 showed interactions with SLR1 or SUMO1($_{GG-AA}$)::SLR1.
373
374 **DISCUSSION**
375 DELLA proteins are central regulators of plant productivity and stress
376 responses, and the hormonal crosstalk mediated by these proteins is essential for
377 plant plasticity to endure stress. As other hormone modulators, DELLA activity is
378 regulated by post-translational modifications, such as ubiquitination, phosphorylation,
379 *O*-fucosylation, *O*-GlcNAcylation, and SUMOylation (Yano et al., 2019; Zentella et al.,
380 2016; Zentella et al., 2017; Conti et al., 2014; Dai and Xue, 2010; Itoh et al., 2003).
381 Recently, SUMO proteases were linked to salt stress response in rice (Srivastava et
382 al., 2016b; 2017). Although deSUMOylation was proposed as a general mechanism
383 of tolerance acquisition in response to salt, we show that artificially SUMOylated SLR1
384 could alleviate the salt stress impact on rice productivity, also improving recovery after
385 stress imposition is released.
386 Following the evidence that SUMO proteases are important for DELLA activity
387 (Campanaro et al., 2016), the knockout mutant of SUMO protease *fug1* showed a
388 higher ratio of overall SUMOylated SLR1. Interestingly, the FUG subclass is
389 phylogenetically close to the SPF subclass, which contains Ulp2-like SUMO proteases
390 (Castro et al., 2018). A Ulp2 from *Saccharomyces cerevisiae* (ScUlp2) was previously
391 reported to be the key protease responsible for poly-SUMO chain processing (Eckhoff
392 and Dohmen, 2015). If FUG1 is indeed related to Ulp2 proteases and it processes
393 SUMO-SLR1, SLR1 deSUMOylation may be occurring in poly-SUMO chain high
394 molecular weight conjugates.
395 DELLA proteins control several plant processes through interaction with a
396 myriad of transcriptional factors (Van De Velde et al., 2017). By affecting protein-
397 protein interaction, SLR1 SUMOylation has the potential to modulate plant processes

398 by altering the transcriptional outcome of SLR1-TFs interacting proteins. Indeed,
399 transcriptomic analysis of SUMOylated SLR1 overexpressing lines suggested that this
400 isoform plays a role in early transcriptional responses to salt stress, affecting the
401 expression of key genes coding for enzymes controlling the accumulation of active
402 GA, such as *GA20ox2* and *GA2ox3*, involved in activation and inactivation of the active
403 GA_4. We were able to determine that SLR1 SUMOylation occurs in lysine 2 (Figure
404 1A-C), distant from the conserved GA regulatory domains DELLA and TVHYNP. This
405 finding suggests that SLR1 SUMOylation contrasts with Arabidopsis RGA, in which
406 the amino acid residue responsible for SUMO modification is the lysine 65 (Conti et
407 al., 2014), located very close to the GA-regulatory domain TVHYNP. The location of
408 SUMO attachment in SLR1 protein could exert quite different effects on protein-protein
409 interactions compared to its well-described Arabidopsis counterpart RGA. An
410 interesting possibility is that SUMOylation of these residues could have a different
411 outcome regarding the transcriptional activation properties of SLR1 DELLA/TVHYNP
412 motifs (Hirano et al., 2012). Both lysines are within SUMOylation canonical motifs, but
413 while the SUMOylation canonical motif surrounding K2 is conserved in all analysed
414 DELLAs, the one containing K65 is exclusive to RGA. The different SUMOylation sites
415 of SLR1 and RGA might account for alterations in DELLA regulation amongst species
416 that probably determine different interactome networks.
417 The SUMOylation of SLR1 could also be affecting the interaction with upstream
418 regulatory proteins. For instance, SUMO attachment could affect SLR1 interaction with
419 SPY, which enhances SLR1 activity through *O*-fucosylation and is a major determinant
420 of rice plant architecture (Yano et al., 2019). Crosstalk between SUMOylation and *O*-
421 fucosylation could play a role in GA-promoted growth regulation by decreasing TF-
422 interactions that result in growth repression (Camut et al., 2017). This control of the
423 expression of GA enzymes is demonstrated by our transcriptomic results of
424 SUMO1SLR1-OX lines under salt stress, which shows upregulation of both *GA20ox2*
425 and *GA2ox3*, suggesting that SLR1 SUMOylation could also regulate GA
426 homeostasis. The induction of genes involved in both anabolism and catabolism of
427 bioactive GA, catalized by GA20ox2 and GA2ox3, respectivelly, seems paradoxical.
428 However, each gene could be activated in different tissues under salt stress,
429 determining tissue specific expression and regulating plant plasticity. These
430 differences in spatial expression are lost in whole plant transcriptomic analysis.

431 Further experiments evaluating *GA20ox2* and *GA2ox3* spatial expression under salt
432 stress have to be done to address the issue.
433 SUMOylation of specific targets was suggested to be crucial for stress
434 tolerance, fertility and yield maintenance in rice. For instance, bZIP23 SUMOylation
435 levels are modulated by OTS1, which affects its stability and the plant's ability to deal
436 with drought and salt stress (Srivastava et al., 2017). Interestingly, we found that
437 bZIP23 interacts with both SLR1 and SUMO1SLR1. Another novel interaction with
438 both bHLH089 and bHLH094 shows upregulation of JAZ-like repressors like JAZ8,
439 consistent with findings that this TF is regulating genes from the JA pathway as
440 observed in our transcriptomic analysis. Both these interactions may partly explain the
441 JA-induced stress response promoted by SLR1 accumulation (Supplemental Figures
442 S7A and S7B).
443 It was already shown that YAB4 interacts with SLR1 to repress *GA20ox2* gene
444 expression and restrain development in rice (Yang et al., 2016). We confirmed the
445 interaction between SLR1 and YAB4 by Y2H assays and BiFC (Figure 5B-C). We
446 additionally show that SUMOylation of SLR1 abolished its interaction with YAB4.
447 Accordingly, we found a stress-induced upregulation of *GA20ox2* in SUMO1SLR1-OX
448 (Supplemental Table S1). Moreover, *GA20ox2* was also found to be downregulated
449 by KNOTTED1-like homeobox (KNOX) proteins like OSH1 (Sakamoto et al., 2006).
450 SLR1 SUMOylation also disrupted its interaction with OSH1, suggesting that SLR1
451 SUMOylation mechanistic action is partly achieved through SLR1 dissociation from
452 transcriptional regulators involved in GA signalling and stress signalling. It could
453 represent a dissociation of DELLA function during salt stress tolerance from its impact
454 on productivity by means of SUMOylation.
455 The emergence of SUMOylation of SLR1 as an effector of rice tolerance to salt
456 stress, through the growth-maintaining modulation of protein-protein interaction with
457 transcriptional regulators such as YAB4, is evidence of the tight regulation of the GA
458 pathway by rice DELLA during stress. Recent studies have demonstrated that DELLA
459 proteins are targets of different post-translational modifications, which could adjust
460 their interactions with transcriptional regulators in a dynamic fashion, ensuring the best
461 developmental decisions when facing stress. Further studies need to be performed to
462 unveil upstream effectors that perceive stress and the underlying signal transduction
463 pathway that leads to SLR1 SUMOylation. By establishing the trigger for SLR1
464 SUMOylation and its effect on stress-induced SLR1 protein-protein interactions, new

465 strategies can be developed involving the transient post-translational modification of
466 DELLA, as mutagenesis and selection of growth-favourable SLR1 alleles. This can be
467 used to activate the SUMO-regulated tolerance mechanism when stress is
468 forthcoming and protect crops from yield losses due to abiotic stress.
469
470 **METHODS**
471 **SLR1 genomic DNA cloning and vectors construction**
472 The intronless gene SLR1 entire coding sequence was amplified from Nipponbare
473 wild-type genomic DNA, using the primers SLR1-CDS-Fw and SLR1-CDS-Rv
474 (Supplemental Table S4). The fragment was cloned into the pJET 1.2/blunt-end
475 cloning vector (ThermoScientific), and the SLR1 full sequence confirmed by Sanger
476 sequencing. SLR1 CDS was then amplified from pJET-SLR1 using the primers pET-
477 Fw-*Eco*RI and pET-Rv-*Psp*OMI (Supplemental Table S4) to insert the restriction sites
478 for *Eco*RI and *Psp*OMI to clone SLR1 in the pET28a expression vector (Novagen). For
479 the generation of rice transgenic lines overexpressing SLR1, the SLR1 coding
480 sequence was amplified from pJET-SLR1 using OsSLR1-GW-Fw and OsSLR1-GW-
481 Fw primers to insert the attB1 and attB2 recombination sites. The amplified PCR-
482 product was recombined into the pDONR221 (ThermoFisher).The SUMO1SLR1 gene
483 fusion was generated using high-fidelity PCR (Phusion DNA Polymerase; NEB)
484 essentially as described in Atanassov et al. (2009). Primers overlapping both the
485 OsSUMO1 3'-end and OsSLR1 5'-end OL-SLR1+SUMO1-3'-Fw and OL
486 SUMO1+SLR1-5'-Rv, were used in combination with OsSLR1-Gw-Rv and OsSUMO1-
487 GW-Fw, respectively, to generate the fragments to be fused. In the next step, the PCR
488 products were purified and used in the fusion PCR reaction containing the OsSUMO1-
489 GW-Fw and OsSLR1-Gw-Rv primers for the final amplification of the final fusion
490 product (Supplemental Table S4). The gene fusions were confirmed by Sanger
491 sequencing. To obtain rice transgenic plant lines overexpressing SLR1 (SLR1-OX)
492 and SLR1 fused to SUMO1 (SUMO1SLR1-OX), pDONR221 containing the inserts
493 described above was used as entry vector for the pANIC6B destination vector (Mann
494 et al., 2011). The expression of SLR1 and SUMO1SLR1 is controlled by the maize
495 *ZmUbi1* promoter (Figure 3A).
496
497 **Site-directed mutagenesis**

498 For the production of truncated recombinant SLR1 protein (SLR1t) containing the
499 leading 190 amino acid residues of SLR1, a stop codon was introduced by site-
500 directed mutagenesis (SDM) in pET28a-SLR1 using *Pfu*Turbo DNA polymerase
501 (Agilent) and the primers (SLR1t-STOP-Fw and SLR1t-STOP-Rv) designed with
502 QuickChangeII online tool (Agilent) (Supplemental Table S4). Unmodified plasmids
503 were digested with methylation-sensitive enzyme *Dpn*I (New England Biolabs). The
504 mutated plasmids were transformed in *E. coli* DH5α and the mutagenized site
505 confirmed by sequencing. Mutated pET28a coding the truncated SLR1 isoform
506 (SLR1t) was subjected to further mutagenesis procedures to perform the amino acid
507 substitutions K2R and K60R (primers SLR1t-K2R-Fw, SLR1t-K2R-Rv, SLR1t-K60R-
508 Fw and SLR1t-K60R-Rv, all listed in Supplemental Table S4) following the same
509 protocol.
510
511 **Recombinant Protein Production and Purification**
512 pET28a vectors containing the full-length SLR1, N-terminus truncated SLR1 (SLR1t),
513 SLR1t (K2R) and SLR1t (K60R) were transformed into *E. coli* strain BL21 Star (DE3,
514 Sigma-Aldrich) for recombinant protein expression. Cells were grown at 37ºC until
515 OD_{600} = 0.6, and protein production was induced by addition of 200 µM isopropyl-d-1-
516 thiogalactopyranoside (IPTG). After three hours, the cells were harvested by
517 centrifugation in a J2MI centrifuge (Beckman) at 7000 RPM during 20 minutes at 4ºC.
518 The cells were resuspended in lysis buffer (phosphate buffer 20 mM pH 7.5, 500 mM
519 NaCl, 10 mM Imidazole) containing 5 µg/mL of DNAse, 50 µg/mL of lysozyme, PMSF
520 100 mM and $MgCl_2$ 25 mM. After freezing at -20ºC and thawing, extracts were loaded
521 into a HisTrap chelating column (Amersham Biosciences) and proteins eluted in
522 phosphate buffer containing 500 mM imidazole, following buffer exchange dialysis
523 (phosphate buffer 20 mM, NaCl 150 mM, DTT 1 M, glycerol 2%), for increased protein
524 stability. Recombinant proteins were analysed by Western Blot using custom-made
525 SLR1 specific polyclonal antibody with Mini-Protean II system (Biorad).
526
527 ***In vitro* SUMOylation assays and ULP1 treatment**
528 The *in vitro* SUMOylation assays were performed in 20 µL of SUMOylation reaction
529 buffer (Werner et al., 2009) containing 3 µg of SLR1 recombinant protein, 1 µg of E1-
530 activating enzyme (OsSAE1/ OsSAE2), 0.8 µg of E2-conjugating enzyme (OsSCE1a),

531 0.5 µg of OsSUMO1/2, 0.4 units of creatine phosphokinase, and 10 mM creatine
532 phosphate. Reactions were initiated by adding 1 mM ATP and then incubated at 37ºC
533 for 1 h to 3 h. To confirm SUMOylation specificity, 3 µg of purified SUMO protease
534 ULP1 from *Saccharomyces cerevisiae* (Li and Hochstrasser, 2003) was used for
535 deSUMOylation analysis. SUMO conjugates were analysed by Western Blot with
536 custom anti-SLR1 antibody. For ULP1 treatments, whole plants were ground in liquid
537 N_2 and 100 mg of ground tissue powder were mixed with non-denaturing buffer (Tris-
538 HCl pH 8.0 50 mM, sodium chloride 150 mM, NP-40 1%, sodium deoxycholate 0.5%,
539 SDS 0.1%, EDTA pH 8.0 1 mM, NEM 50 mM), followed by homogenisation by
540 vortexing, and subsequent centrifugation at 4 ºC for 20 minutes to recover the
541 supernatant containing the proteins. The non-denaturing protein extracts were treated
542 with 7 µg of ULP1, incubated at 37 ºC with collection points taken at 5, 30, 60, and
543 120 seconds. Proteins were denatured at 90ºC for 10 minutes with Laemmli Buffer
544 with 5 mM DTT and anti-SLR1 immunoblot proceeded as described above.
545
546 **SLR1 protein extraction, detection and quantification analysis**
547 Plant shoot samples were ground in liquid N_2 and 100 mg of ground tissue used for
548 protein extraction with denaturing TCA/Acetone precipitation, followed by
549 resuspension in lysis buffer (7 M Urea, 2 M Thiourea, 30 mM Tris, 4% (w/v) CHAPS,
550 4 % (v/v), cOmplete protease inhibitor cocktail EDTA-Free (Sigma-Aldrich), 0.1% (v/v)
551 Nuclease Mix 100x, and NEM 20 mM. Protein quantification was performed with 2-D
552 Quant kit (GE Healthcare) following manufacturer's instructions. Anti-SLR1
553 immunoblots were performed in a Mini-Protean II System (Biorad), using custom-
554 made anti-SLR1 polyclonal specific antibody [1:5.000, overnight incubation] and anti-
555 rabbit (Novex) [1:20.000, 90 min incubation] in 5% non-fat dry milk in TBS 1X.
556 Quantification of native SLR1 bands provided by immunoblotting analysis, normalized
557 to protein loading control using stripped membrane stained with Coomassie G-250
558 (Fluka), was performed with ImageJ software as indicated in the official ImageJ
559 website online tutorial.
560
561 **Plant material and Rice transformation**
562 Calluses induced from wild-type *Oryza sativa* (japonica spp.) cv. Nipponbare mature
563 seeds were used for rice transformations according to (Almadanim et al., 2017), and
564 selection for transformants asserted by hygromycin resistance and standard GUS-

565 staining with X-Gluc solution (Roth) of a section of seminal roots. Proteins were
566 extracted, detected and quantified using a modified TCA/Acetone method (Luís et al.,
567 2016). Due to growth arrest phenotype and fertility decrease in homozygous lines of
568 SUMO1SLR1-OX lines, all assays continued with positively-selected heterozygous
569 plants. Moreover, lines #2 for both SUMO1SLR1-OX and SLR1-OX were selected for
570 further analysis at rice booting stage and transcriptomic evaluation according to non-
571 SUMOylated SLR1 levels, in order to avoid DELLA pleiotropic effects (Davière and
572 Achard, 2015). Wild-type Nipponbare was used as a control for SLR1-OX and
573 SUMO1SLR1-OX obtained by transformation as described above. Negative segregant
574 lines of Zhonghua and Hwayoung varieties were used as controls for T-DNA insertion
575 lines knock-out mutants for rice SUMO proteases ELS1 (04Z11JY66) and FUG1 (2A-
576 20225 obtained from RMD (www.rmd.ncpgr.cn), developed by the National Centre of
577 Plant Gene Research) and Postech (www.postech.ac.kr/life/pfg/risd, developed by
578 Gynheung An), respectively. These insertion line seeds were germinated, self-crossed
579 and screened using PCR analysis for homozygosity (Rosa et al., 2018). The T-DNA
580 insertion position was determined by sequencing. Gene expression was analysed by
581 RT-qPCR (Rosa et al., 2018).
582
583 **Salinity Stress Assays**
584 For the assays performed at the seedling stage, heterozygous transgenic seeds were
585 germinated and selected through screening for hygromycin resistance and GUS
586 staining. Seedlings were transferred to hydroponics for salinity resistance screening
587 (Almeida et al., 2016) with half-strength Murashige & Skoog Medium and MES buffer
588 250 mg/L (Duchefa) with pH adjusted to 5.2. Seedlings were grown for 14 days before
589 the salt stress assay. Then, the seedlings were exposed to salt stress, with electric
590 conductivity (EC) set and maintained at 12 dS/m with sodium chloride solution for the
591 extension of the stress treatment. After 8 days, the seedlings were transferred to
592 regular medium for recovery. Stress severity (SES score) – 1 for lower severity and 9
593 for higher severity - was evaluated as set by IRRI (Gregorio et al., 1997) at 6 and 8
594 days after stress and 8 days after recovery. Samples for transcriptomic analysis – 4
595 replicates of a pool of 3 plants - were collected at 8 hours after the initiation of the salt
596 stress, corresponding to 10 hours after the lights went on, for both control and salt
597 treatments, and frozen immediately in liquid nitrogen for grinding and analysis.
598 Samples from 0h, 2h, 4h, and 8h treatments were obtained from shoots and roots

599 collected separately, and frozen immediately in liquid nitrogen. Protein was extracted,
600 detected and quantified as described above. For the booting stage assay, previously
601 germinated and selected heterozygous transgenic seeds were sown in pots with 2-
602 parts soil, 2-parts peat, and 1-part vermiculite. The experiment was set up in the
603 greenhouse from June to September, according to IRRI standard screening
604 procedures (Gregorio et al., 1997). Genotypes were maintained in separate
605 containers, for both stress and control pots, to control for discrepancies in panicle
606 initiation times. Panicle initiation was evaluated by the emergence of the flag-leaf with
607 a distance between 1 and 2 cm to the adjacent leaf and salinity applied individually for
608 each genotype at that point. Electric conductivity (EC) was set and maintained at 8
609 dS/m with sodium chloride solution for the extension of the life cycle. Upon complete
610 maturation of the seed, agronomical parameters were measured (plant height, tillering,
611 and panicle length) and panicles collected for further characterization of fertility
612 (analysing the number of full matured seeds to total number of flowers ratio) and
613 productivity (weight of 1000 seeds as measured in a Pfeuffer seed counter). The
614 significance of statistics was asserted by t-test with Holm-Sidak method correction for
615 multiple comparisons and a $p<0.05$ threshold.
616
617 **RNA Extraction and expression analysis**
618 RNA was extracted from a total of 100 mg of ground frozen shoot tissue with Direct-
619 zol kit (Zymo Research) according to manufacturer's protocol with in-column DNAse
620 treatment. The first-strand cDNA was synthesized from 2 µg of total RNA with an
621 anchored-oligo (dT)18 primer using the Transcriptor High Fidelity cDNA Synthesis Kit
622 (Roche) according to the manufacturer's instructions. Reverse Transcription
623 quantitative PCR (RT- qPCR) analysis was performed using a LightCycler 480 system
624 (Roche) and the SYBR Green I Master mix (Roche). The RT-qPCR reactions were
625 carried out with the primers listed in Supplemental Table S4. PCR running conditions
626 were: one cycle at 95ºC for 5 min and 45 cycles of amplification at 95ºC for 10 s, 56–
627 60ºC for 10 s and 72ºC /10 s. The CT values were calculated using three technical
628 replicates, and gene expression was assessed relative to described internal reference
629 transcript controls, rice *UBIQUITIN CONJUGASE2* (OsUBC2) and *UBIQUITIN10*
630 (OsUBQ10) (Moraes et al., 2015; Pabuayon et al., 2016). For the RNA-seq procedure,
631 the small RNAs in the extracted total RNA samples were cleaned by using the RNeasy
632 spin column from RNeasy Mini Kit (Qiagen) following RNA Cleanup protocol. RNA

633 quality was assessed by Fragment Analyzer (ThermoFisher) with RNA Quality
634 Number over 5. A total of 18 cDNA libraries were prepared, using three biological
635 replicates for each genotype (SLR1-OX, SUMO1SLR1-OX, Nipponbare) and each
636 condition (mock and salt). Enzymatic fragmentation with Pico Nextera kit and Smart-
637 Seq2 multiplexed-library preparation were performed[49] and single-end sequencing on
638 NextSeq500 (Illumina) with High Output Kit (75 cycles).
639
640 **RNA-seq Data Analysis**
641 Raw data FASTQ files were inputted on R/Bioconductor-based user interface analysis
642 software Chipster for RNA-seq. Single-end reads were trimmed with PRINSEQ for 55
643 bp total with 18 bp trimmed on 5' end and quality control of 28% set for the 3' end for
644 adapter removal. Read alignment was performed with TOPHAT2 against the *Oryza*
645 *sativa* genome (version IRGSP-1.0.36), selecting Sanger-Phred +33 as quality score
646 format. An average of 25.000.000 and 21.000.000 aligned and uniquely mapped
647 reads, respectively, were obtained per library (Supplemental Table S2). For differential
648 expression analysis, BAM files resulting from alignment were submitted to pairwise
649 comparisons with Cufflinks2 tool Cuffdiff for a set 0.05 False Discovery Rate (5% FDR)
650 with sequence-specific bias and multi-mapped read corrections enabled. Differentially
651 expressed genes (DEGs) with a 1.5 fold-change were selected for data visualization
652 and functional annotation using ClueGO plug-in (Bindea et al., 2009) for Cytoscape
653 (Su et al., 2014).
654
655 **Promoter Analysis and Interaction Validation by Y2H and BiFC**
656 The 1000 bp promoter region of differential expressed genes DEGs were downloaded
657 from Rice Annotation Project Database (RAP-DB) (Sakai et al., 2013) and submitted
658 to PlantPAN 2.0 (Chow et al., 2016) for *cis*-elements for transcription factor binding
659 site (TFBS) analysis. Gene Group Analysis was used to search for common (90%)
660 *cis*-element binding (TFBS) sites and the transcription factors (TFs) associated with
661 DEG promoters. Rice TFs were examined individually for experimentally verified data
662 concerning the interaction to binding sites and downstream target genes listing
663 (Supplemental Table S2). Resulting target genes were then overlapped with
664 previously verified DEGs from RNA-seq analysis. For the Y2H assays, coding
665 sequences of SLR1 and OsSUMO1($_{GG\text{-}AA}$)::SLR1 were cloned into the pGADT7 vector
666 (Stratagene, USA) while OsbHLH089, OsbHLH094, OsbZIP23, OsIDEF1, OsOSH1,

667 OsPCF1 and OsYAB4 were cloned into the pGBKT7 (Stratagene, USA) vector. These
668 constructs were transformed into *Saccharomyces cerevisiae* strain Y2HGold
669 (Clontech, US) applying the LiAc method. Yeast transformed cells were plated on
670 synthetic defined (SD) medium lacking leucine and tryptophan for plasmid
671 transformation control and in SD lacking leucine (-Leu), tryptophan (-Trip), adenine (-
672 Ade), and histidine (-His) for interaction screening. The interactions were evaluated in
673 three individual colonies transformed with both plasmids. pAD-WT and pBD-WT from
674 the HybriZAP 2.1 kit (Stratagene, USA) were used as a control of positive interaction
675 (C+). pGBKT7 and pGADT7 empty vectors were also co-transformed with pGADT7-
676 SLR1, pGADT7-SUMO1($_{GG-AA}$)::SLR1 and pGBKT7-bHLH089, pGBKT7-bZIP23,
677 pGBKT7-IDEF1, and pGBKT7-YAB4, respectively, as negative controls. For
678 bimolecular fluorescence complementation (BiFC), OsSLR1, OsSUMO1($_{GG-AA}$)::SLR1
679 were cloned in YFN43, and OsbHLH089, OsbHLH094 and OsYAB4 were cloned into
680 YFC43 (Belda-Palazón et al., 2012). *Nicotiana benthamiana* leaves were co-infiltrated
681 with *Agrobacterium tumefaciens* strain EH105 harbouring the appropriate vectors.
682 Fluorescence was visualized using the Leica DM6 B fluorescence microscope (40x)
683 with L5 filter cube (Leica, Germany) 48-72h following infiltration. As negative control,
684 YFN43 (empty vector) was also co-infiltrated with YFC43-bHLH089, YFC43-bHLH094
685 and YFC43-YAB4. *Agrobacterium* expressing the viral silencing suppressor P19 was
686 included in all infiltrations to increase the expression in *N. benthamiana* leaves. BiFC
687 analyses were performed essentially as described in Belda-Palazón et al., 2012.
688

689 **Accession Numbers**

690 Sequence data from this article can be found in the Rice Annotation Project Database
691 (RAP-DB) under the following accession numbers: OsSLR1 (Os03g0707600),
692 OsSUMO1 (Os01g0918300), OsSUMO2 (Os01g0918200), OsSAE1
693 (Os11g0497000), OsSCE1a (Os03g0123100), OsELS1 (Os01g0355900), OsFUG1
694 (Os03g0344300), OsUBC2 (Os02g0634800), OsUBQ10 (Os06g0681400), OsP5CS
695 (Os05g0455500), OsRAB21 (Os11g0454300), RGA (At2g01570), OsCPS4
696 (Os04g0178300), OsKSL7 (Os02g0570400), OsCYP701A8/KO1 (Os06g0569500),
697 OsCYP99A3 (Os04g0178400), OsCYP71Z6 (Os02g0570500), OsCYP76M8
698 (Os02g0569400), OsCYP71Z7 (Os02g0570700), OsCKX2 (Os01g0197700),
699 OsCKX5 (Os01g0775400), OsLOX2 (Os08g0509100), OsCHT3 (Os06g0726100),
700 OsCHT8 (Os10g054290), OsCHT11 (Os03g0132900), OsGA20ox2

701 (Os01g0883800), OsGA2ox3 (Os01g0757200), OsPCF1 (Os04g0194600),
702 OsRISBZ3 (Os02g0266800), OsbHLH089 (Os03g0802900), OsbHLH094
703 (Os07g0193800), OsbZIP23 (Os02g0766700), OsOSH1 (Os03g0727000), OsPCF1
704 (Os03g0785800), OsIDEF1 (Os11g0175700), OsYAB4 (Os02g0643200).
705
706

Supplementary Materials

Figure S1. Alignment of DELLAs protein sequences of selected monocots and dicots.
Figure S2. SRL1 can be SUMOylated by both OsSUMO1 and OsSUMO2 *in vitro.*
Figure S3. Accumulation dynamics of SRL1 transcript and protein in response to salt stress.
Figure S4. Tillering and panicle length were not affected by mild salt stress imposition.
Figure S5. Analysis of salt treatment efficiency by salt-stress marker gene induction.
Figure S6. Salt treatment had a major contribution to the differences in gene expression among Nipponbare, SLR1-OX and SUMO1SLR1-OX.
Figure S7. Transcriptomics reveal differential stress-induced regulation by SUMOylated SLR1.
Figure S8. Protein-protein interaction (PPI) negative controls for Y2H and BiFC assays.
Figure S9. Genevestigator Results for Gene Expression of YABBY4 (LOC_Os02g4950) in Salinity Assays.
Table S1. RNA seq data showing >1.5 fold Differentially Expressed Genes in Nipponbare, SLR1-OX and SUMOSLR1-OX, in mock and salt stress conditions.
Table S2. Expression changes of selected putative SLR1 TF interactors (A) and the respective downstream target genes (B). Fold-change shown as $\log_2$ FC. Comparison of condition A with condition B corresponding to respective selected analysis in Cufflinks (FPKM1 x FPKM2, for condition A and B, respectively). Nipp-Nipponbare; (m)-mock; (s)-stress
Table S3. RNA-seq read count for each of the sequenced libraries and respective legend
Table S4. List of primers used for gene cloning, site directed mutagenesis (SDM) and gene expression quantification (RT-qPCR). Details for the use of specific primers are given in the text.

Acknowledgments

Portuguese Fundação para a Ciência e a Tecnologia (FCT) for fellowships for NMG (SFRH/BD/85799/2012), TF (PD/BD/135584/2018), MTGR (SFRH/BD/84219/2012), MAAR (SFRH/BD/87420/2012), PMB (SFRH/BPD/86742/2012). FCT Investigator IF/00764/2014 (POPH-QREN) for IAA and PTDC/BIA-FBT/31211/2017 for CM contract. Work was supported by P-KBBE/0001/2012 and also by the FCT research unit GREEN-it "Bioresources4sustainability" (UID/Multi/04551/2013 and UIDB/04551/2020). The funding sources had no involvement in study design, analyses, and interpretation of data, writing, or in the submission decision.

Table 1. Enriched binding sites and associated transcription factors in SLR1 DEGs promoters. Promoter sequence analysis output from PlantPAN with Support referencing the percentage of transcription factor binding elements (TFBS/Sequence) found in SLR1- and SUMO1SLR1-dependent stress-responsive DEGs. Resulting TF overlap with DEGs detailed in Supplementary Table S4.

TFBS	Support	TF Family	TF	Annotation
GGTCCCAC	91.4	**TCP**	**PCF1/2**	essential for meristematic tissue-specificity expression of the PCNA gene promoter
TACGTA	91.4	**(Others)**	**RISBZ3**	found in seed storage protein gene promoters
GCACGTGC	94.7	**bHLH**	**BHLH089/094**	forms a ternary complex with RSS3 and TIFY11A/JAZ9 to negatively regulate jasmonate-responsive genes
ACACGTGT	97.4	**bZIP**	**BZIP23/46**	binds specifically to the abiotic stress ABA-responsive elements (ABRE) in the promoter of target genes
TNCGTACAA	98.0	**SBP**	**SPL1**	trans-acting factor that binds specifically to the consensus nucleotide sequence 5'-TNCGTACAA-3'
TGAC	98.7	**Homeobox**	**OSH1**	involved in shoot formation during embryogenesis
CATGC	100.0	**B3**	**IDEF1**	involved in iron deficiency response and tolerance
CCAAT	100.0	**NF-YB**	**NFBY1/2/3/4**	component of the NF-Y/HAP transcription factor complex regulating the expression of photosynthetic genes

REFERENCES

- Achard, P., Cheng, H., De Grauwe, L., Decat, J., Schoutteten, H., Moritz, T., Van Der Straeten, D., Peng, J., and Harberd, N.P. (2006). Integration of plant responses to environmentally activated phytohormonal signals. Science *311*, 91–94.
- Almadanim, M.C., Alexandre, B.M., Rosa, M.T.G., Sapeta, H., Leitão, A.E., Ramalho, J.C., Lam, T.T., Negrão, S., Abreu, I.A., and Oliveira, M.M. (2017). Rice calcium-dependent protein kinase OsCPK17 targets plasma membrane intrinsic protein and sucrose-phosphate synthase and is required for a proper cold stress response. Plant Cell Environ. *40*, 1197–1213.
- Almeida, D.M., Almadanim, M.C., Lourenço, T., Abreu, I.A., Saibo, N.J.M., and Oliveira, M.M. (2016). Screening for Abiotic Stress Tolerance in Rice: Salt, Cold, and Drought. In Environmental Responses in Plants, (New York, NY: Humana Press, New York, NY), pp. 155–182.
- Atanassov, I.I., Atanassov, I.I., Etchells, J., and Turner, S.R. (2009). A simple, flexible and efficient PCR-fusion/Gateway cloning procedure for gene fusion, site-directed mutagenesis, short sequence insertion and domain deletions and swaps. Plant Methods 2009 5:1 *5*, 14.
- Augustine, R.C. and Vierstra, R.D. (2018). SUMOylation: re-wiring the plant nucleus during stress and development. Current opinion in plant biology, 45, pp.143-154.
- Belda-Palazón, B., Ruiz, L., Martí, E., Tárraga, S., Tiburcio, A.F., Culiáñez, F., Farràs, R., Carrasco, P. and Ferrando, A. (2012). Aminopropyltransferases involved in polyamine biosynthesis localize preferentially in the nucleus of plant cells. PLoS One, 7(10), p.e46907.
- Bindea, G., Mlecnik, B., Hackl, H., Charoentong, P., Tosolini, M., Kirilovsky, A., Fridman, W.-H., Pagès, F., Trajanoski, Z., and Galon, J. (2009). ClueGO: a Cytoscape plug-in to decipher functionally grouped gene ontology and pathway annotation networks. Bioinformatics *25*, 1091–1093.
- Campanaro, A., Battaglia, R., Galbiati, M., Sadanandom, A., Tonelli, C., and Conti, L. (2016). SUMO proteases OTS1 and 2 control filament elongation through a DELLA-dependent mechanism. Plant Reprod *29*, 1–4.
- Camut, L., Davière, J.-M., and Achard, P. (2017). Dynamic Regulation of DELLA Protein Activity: SPINDLY and SECRET AGENT Unmasked! Mol Plant *10*, 785–787.
- Castro, P.H., Bachmair, A., Bejarano, E.R., Coupland, G., Lois, L.M., Sadanandom, A., van den Burg, H.A., Vierstra, R.D., and Azevedo, H. (2018). Revised nomenclature and functional overview of the ULP gene family of plant deSUMOylating proteases. J. Exp. Bot. *69*, 4505–4509.
- Chow, C.-N., Zheng, H.-Q., Wu, N.-Y., Chien, C.-H., Huang, H.-D., Lee, T.-Y., Chiang-Hsieh, Y.-F., Hou, P.-F., Yang, T.-Y., and Chang, W.-C. (2016). PlantPAN 2.0: an update of plant promoter analysis navigator for reconstructing transcriptional regulatory networks in plants. Nucleic Acids Research *44*, D1154–D1160.
- Conti, L., Nelis, S., Zhang, C., Woodcock, A., Swarup, R., Galbiati, M., Tonelli, C., Napier, R., Hedden, P., Bennett, M., et al. (2014). Small Ubiquitin-like Modifier protein SUMO enables plants to control growth independently of the phytohormone gibberellin. Developmental Cell *28*, 102–110.
- Cremona, C.A., Sarangi, P., and Zhao, X. (2012). Sumoylation and the DNA Damage Response. Biomolecules 2012, Vol. 2, Pages 376-388 *2*, 376–388.

- Crozet, P., Margalha, L., Butowt, R., Fernandes, N., Elias, C.A., Orosa, B., Tomanov, K., Teige, M., Bachmair, A., Sadanandom, A., et al. (2015). SUMOylation represses SnRK1 signaling in Arabidopsis. The Plant Journal *85*, 120–133.
- Dai, C., and Xue, H.-W. (2010). Rice early flowering1, a CKI, phosphorylates DELLA protein SLR1 to negatively regulate gibberellin signalling. The EMBO Journal *29*, 1916–1927.
- Davière, J.-M., and Achard, P. (2015). A pivotal role of DELLAs in regulating multiple hormone signals. Mol Plant *9*, 10–20.
- de Lucas, M., Daviere, J.M., Rodriguez-Falcon, M., Pontin, M., Iglesias-Pedraz, J.M., Lorrain, S., Fankhauser, C., Blazquez, M.A., Titarenko, E., and Prat, S. (2008). A molecular framework for light and gibberellin control of cell elongation. Nature 451, 480-484.
- Eckhoff, J., and Dohmen, R.J. (2015). In Vitro Studies Reveal a Sequential Mode of Chain Processing by the Yeast SUMO (Small Ubiquitin-related Modifier)-specific Protease Ulp2. J. Biol. Chem. *290*, 12268–12281.
- Fukazawa, J., Mori, M., Watanabe, S., Miyamoto, C., Ito, T., and Takahashi, Y. (2017). DELLA-GAF1 Complex Is a Main Component in Gibberellin Feedback Regulation of GA20 Oxidase 2. Plant Physiology *175*, 1395–1406.
- Gregorio, G.B., Senadhira, D., and Mendoza, R.D. (1997). Screening rice for salinity tolerance. Irri.
- Hedden, P., and Thomas, S.G. (2012). Gibberellin biosynthesis and its regulation. Biochemical Journal *444*, 11–25.
- Hirano, K., Asano, K., Tsuji, H., Kawamura, M., Mori, H., Kitano, H., Ueguchi-Tanaka, M., and Matsuoka, M. (2010). Characterization of the molecular mechanism underlying gibberellin perception complex formation in rice. The Plant Cell Online *22*, 2680–2696.
- Hirano, K., Ueguchi-Tanaka, M., and Matsuoka, M. (2008). GID1-mediated gibberellin signaling in plants. Trends Plant Sci *13*, 192–199.
- Hirano, K., Kouketu, E., Katoh, H., Aya, K., Ueguchi-Tanaka, M. and Matsuoka, M. (2012). The suppressive function of the rice DELLA protein SLR1 is dependent on its transcriptional activation activity. The Plant Journal, 71(3), pp.443-453.
- Hruz, T., Laule, O., Szabo, G., Wessendorp, F., Bleuler, S., Oertle, L., Widmayer, P., Gruissem, W. and Zimmermann, P. (2008). Genevestigator v3: a reference expression database for the meta-analysis of transcriptomes. Advances in bioinformatics.
- Itoh, H., Matsuoka, M., and Steber, C.M. (2003). A role for the ubiquitin-26S-proteasome pathway in gibberellin signaling. Trends Plant Sci *8*, 492–497.
- Itoh, H., Sasaki, A., Ueguchi-Tanaka, M., Ishiyama, K., Kobayashi, M., Hasegawa, Y., Minami, E., Ashikari, M., and Matsuoka, M. (2005). Dissection of the phosphorylation of rice DELLA protein, SLENDER RICE1. Plant Cell Physiol. *46*, 1392–1399.
- Li, K., Yu, R., Fan, L.M., Wei, N., Chen, H. and Deng, X.W. (2016). DELLA-mediated PIF degradation contributes to coordination of light and gibberellin signalling in Arabidopsis. Nature communications, 7, p.11868.
- Li, S.-J., and Hochstrasser, M. (2003). The Ulp1 SUMO isopeptidase: distinct domains required for viability, nuclear envelope localization, and substrate specificity. *160*, 1069.
- Luís, I.M., Alexandre, B.M., Oliveira, M.M., and Abreu, I.A. (2016). Selection of an Appropriate Protein Extraction Method to Study the Phosphoproteome of Maize Photosynthetic Tissue. Plos One *11*, e0164387.
- Mann, D.G.J., LaFayette, P.R., Abercrombie, L.L., King, Z.R., Mazarei, M., Halter, M.C., Poovaiah, C.R., Baxter, H., Shen, H., Dixon, R.A., et al. (2011). Gateway-compatible vectors for high-throughput gene functional analysis in switchgrass (Panicum virgatum L.) and other monocot species. - PubMed - NCBI. Plant Biotechnol. J. *10*, 226–236.
- Marín-de la Rosa, N., Pfeiffer, A., Hill, K., Locascio, A., Bhalerao, R.P., Miskolczi, P., Grønlund, A.L., Wanchoo-Kohli, A., Thomas, S.G., Bennett, M.J. and Lohmann, J.U. (2015). Genome wide binding site analysis reveals transcriptional coactivation of cytokinin-responsive genes by DELLA proteins. PLoS genetics, 11(7), p.e1005337.
- Miura, K., Jin, J.B., and Hasegawa, P.M. (2007). Sumoylation, a post-translational regulatory process in plants. Current Opinion in Plant Biology *10*, 495–502.
- Moraes, G.P., Benitez, L.C., do Amaral, M.N., Vighi, I.L., Auler, P.A., da Maia, L.C., Bianchi, V.J., and Braga, E.J.B. (2015). Evaluation of reference genes for RT-qPCR studies in the leaves of rice seedlings under salt stress. Genet. Mol. Res. *14*, 2384–2398.
- Munns, R., and Tester, M. (2008). Mechanisms of salinity tolerance. Annu. Rev. Plant Biol. *59*, 651–681.

857 ○ Negrão, S., Courtois, B., Ahmadi, N., Abreu, I., Saibo, N., and Oliveira, M.M. (2011). Recent
858 Updates on Salinity Stress in Rice: From Physiological to Molecular Responses. Critical
859 Reviews in Plant Sciences *30*, 329–377.
860 ○ Nelis, S., Conti, L., Zhang, C., and Sadanandom, A. (2015). A functional Small Ubiquitin-like
861 Modifier (SUMO) interacting motif (SIM) in the gibberellin hormone receptor GID1 is conserved
862 in cereal crops and disrupting this motif does not abolish hormone dependency of the DELLA-
863 GID1 interaction. Plant Signaling & Behavior *10*, e987528.
864 ○ Otomo, K., Kenmoku, H., Oikawa, H., König, W.A., Toshima, H., Mitsuhashi, W., Yamane, H.,
865 Sassa, T., and Toyomasu, T. (2004). Biological functions of ent- and syn-copalyl diphosphate
866 synthases in rice: key enzymes for the branch point of gibberellin and phytoalexin biosynthesis.
867 Plant J. *39*, 886–893.
868 ○ Pabuayon, I.M., Yamamoto, N., Trinidad, J.L., Longkumer, T., Raorane, M.L., and Kohli, A.
869 (2016). Reference genes for accurate gene expression analyses across different tissues,
870 developmental stages and genotypes in rice for drought tolerance. Rice *9*, 32.
871 ○ Rosa, M.T.G., Almeida, D.M., Pires, I.S., da Rosa Farias, D., Martins, A.G., da Maia, L.C., de
872 Oliveira, A.C., Saibo, N.J.M., Oliveira, M.M., and Abreu, I.A. (2018). Insights into the
873 transcriptional and post-transcriptional regulation of the rice SUMOylation machinery and into
874 the role of two rice SUMO proteases. BMC Plant Biol *18*, 349.
875 ○ Sakai, H., Lee, S.S., Tanaka, T., Numa, H., Kim, J., Kawahara, Y., Wakimoto, H., Yang, C.-C.,
876 Iwamoto, M., Abe, T., et al. (2013). Rice Annotation Project Database (RAP-DB): an integrative
877 and interactive database for rice genomics. - PubMed - NCBI. Plant Cell Physiol. *54*, e6–e6.
878 ○ Sakamoto, T., Sakakibara, H., Kojima, M., Yamamoto, Y., Nagasaki, H., Inukai, Y., Sato, Y., and
879 Matsuoka, M. (2006). Ectopic Expression of KNOTTED1-Like Homeobox Protein Induces
880 Expression of Cytokinin Biosynthesis Genes in Rice. Plant Physiology *142*, 54–62.
881 ○ Sarhadi, E., Bazargani, M.M., Sajise, A.G., Abdolahi, S., Vispo, N.A., Arceta, M., Nejad, G.M.,
882 Singh, R.K., and Salekdeh, G.H. (2012). Proteomic analysis of rice anthers under salt stress.
883 Plant Physiology and Biochemistry *58*, 280–287.
884 ○ Srivastava, A.K., Zhang, C., and Sadanandom, A. (2016a). Rice OVERLY TOLERANT TO SALT
885 1 (OTS1) SUMO protease is a positive regulator of seed germination and root development.
886 Plant Signaling & Behavior *11*, e1173301.
887 ○ Srivastava, A.K., Zhang, C., Caine, R.S., Gray, J., and Sadanandom, A. (2017). Rice SUMO
888 protease Overly Tolerant to Salt 1 targets the transcription factor, OsbZIP23 to promote drought
889 tolerance in rice. The Plant Journal *92*, 1031–1043.
890 ○ Srivastava, A.K., Zhang, C., Yates, G., Bailey, M., brown, A., and Sadanandom, A. (2016b).
891 SUMO is a critical regulator of salt stress responses in rice. Plant Physiology *170*,
892 pp.01530.2015–pp.01530.2391.
893 ○ Su, G., Morris, J.H., Demchak, B., and Bader, G.D. (2014). Biological network exploration with
894 Cytoscape 3. - PubMed - NCBI. Current Protocols in Bioinformatics *47*, 8.13.1–8.13.24.
895 ○ Ueguchi-Tanaka, M., Hirano, K., Hasegawa, Y., Kitano, H., and Matsuoka, M. (2008). Release
896 of the repressive activity of rice DELLA protein SLR1 by gibberellin does not require SLR1
897 degradation in the gid2 mutant. Plant Cell *20*, 2437–2446.
898 ○ Ulrich, H.D. (2008). The fast-growing business of SUMO chains. Mol. Cell *32*, 301–305.
899 ○ Van De Velde, K., Ruelens, P., Geuten, K., Rohde, A., and Van Der Straeten, D. (2017).
900 Exploiting DELLA Signaling in Cereals. Trends Plant Sci.
901 ○ Vanstraelen, M., and Benková, E. (2012). Hormonal interactions in the regulation of plant
902 development. Annu. Rev. Cell Dev. Biol. *28*, 463–487.
903 ○ Werner, A., Moutty, M.-C., Möller, U., and Melchior, F. (2009). Performing in vitro sumoylation
904 reactions using recombinant enzymes. Methods Mol. Biol. *497*, 187–199.
905 ○ Xue, Y., Zhou, F., Fu, C., Xu, Y., and Yao, X. (2006). SUMOsp: a web server for sumoylation site
906 prediction. Nucleic Acids Research *34*, W254–W257.
907 ○ Yang, C., Ma, Y., and Li, J. (2016). The rice YABBY4 gene regulates plant growth and
908 development through modulating the gibberellin pathway. J. Exp. Bot. *67*, erw319–erw5556.
909 ○ Yano, K., Morinaka, Y., Wang, F., Huang, P., Takehara, S., Hirai, T., Ito, A., Koketsu, E.,
910 Kawamura, M., Kotake, K. and Yoshida, S., 2019. GWAS with principal component analysis
911 identifies a gene comprehensively controlling rice architecture. Proceedings of the National
912 Academy of Sciences, 116(42), pp.21262-21267.
913 ○ Yates, G., Srivastava, A.K., and Sadanandom, A. (2016). SUMO proteases: uncovering the roles
914 of deSUMOylation in plants. J. Exp. Bot. *67*, 2541–2548.
915 ○ Zentella, R., Hu, J., Hsieh, W.P., Matsumoto, P.A., Dawdy, A., Barnhill, B., Oldenhof, H.,
916 Hartweck, L.M., Maitra, S., Thomas, S.G. and Cockrell, S. (2016). O-GlcNAcylation of master

growth repressor DELLA by SECRET AGENT modulates multiple signaling pathways in Arabidopsis. Genes & development, 30(2), pp.164-176.

- Zentella, R., Sui, N., Barnhill, B., Hsieh, W.-P., Hu, J., Shabanowitz, J., Boyce, M., Olszewski, N.E., Zhou, P., Hunt, D.F., et al. (2017). The Arabidopsis O-fucosyltransferase SPINDLY activates nuclear growth repressor DELLA. Nat. Chem. Biol. *21*, 985–485.

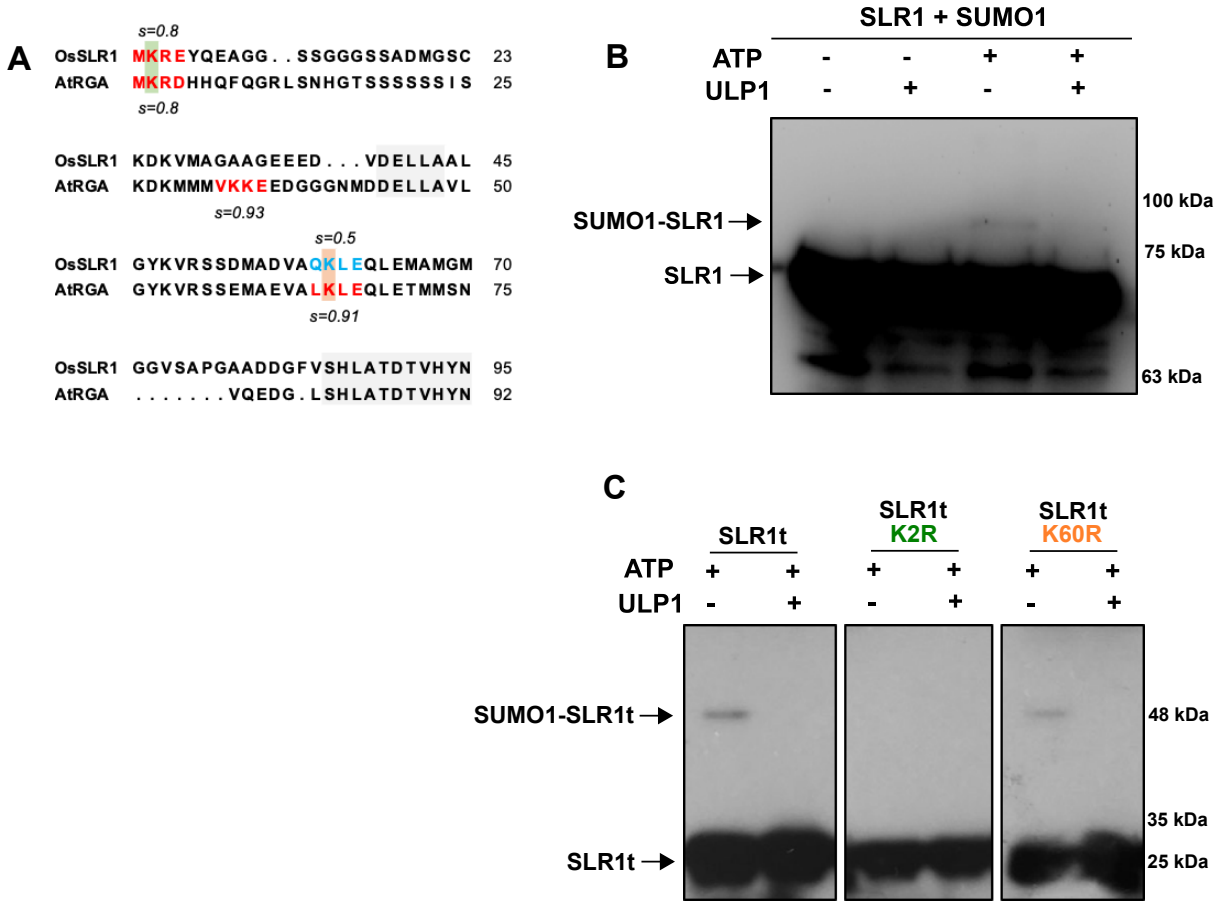

Figure 1. SLR1 is SUMOylated *in vitro* in a novel SUMO-conjugation canonical motif. **(A)** *in silico* prediction of SLR1 canonical motifs (ψ-K-X-E) in the N-terminal region as scored by SUMOsp2 software (Xue et al., 2006), compared to *Arabidopsis thaliana* RGA corresponding region. Motifs showing high SUMOylation probability are marked in red, and low probability motifs are marked in blue. SLR1 K2 and K60 are shown in green and orange, respectively. **(B-C)** *in vitro* SUMOylation assays using rice SUMOylation machinery (OsSCE1, OsSAE1/2, and OsSUMO1) with recombinant SLR1 and SLR1t (SLR1 N-terminal truncated) proteins, treated with ULP1 SUMO protease, as indicated. SLR1 and SLR1t were detected by immunoblotting using custom made anti-SLR1 antibody, where **(B)** corresponds to the full-length SLR1, and **(C)** to the SLR1t coding the leading 190 first SLR1 residues, as well as the mutated isoforms SLR1t K2R and SLR1t K60R.

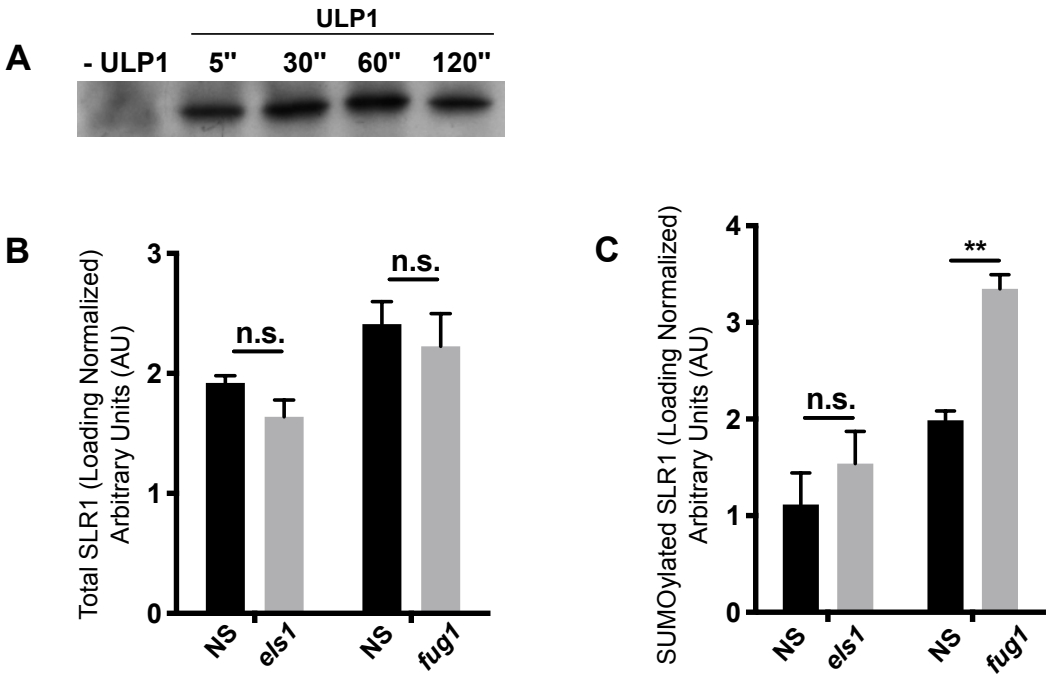

Figure 2. SUMO-specific protease activity reveal SLR1 *in vivo* regulation by SUMO. (A) *Oryza sativa* L. cv Nipponbare non-denaturing protein extracts treated with *Saccharomyces cerevisiae* Ulp1 (ULP1) for SLR1 deSUMOylation analysis as detected by immunoblot using anti-SLR1 antibody. **(B)** Loading-normalized relative quantification of total SLR1 protein in *els1* and *fug1* mutants, and the respective negative segregants (NS) after deSUMOylation by ULP1 treatment**;** and **(C)** total SUMOylated SLR1, as shown by ratio comparison to non-SUMOylated protein after ULP1 treatment. Error bars correspond to standard error (SE; n=4). Statistically significant values are represented as **($p<0.01$). The significance of statistics was asserted by t-test with Holm-Sidak method correction for multiple comparisons.

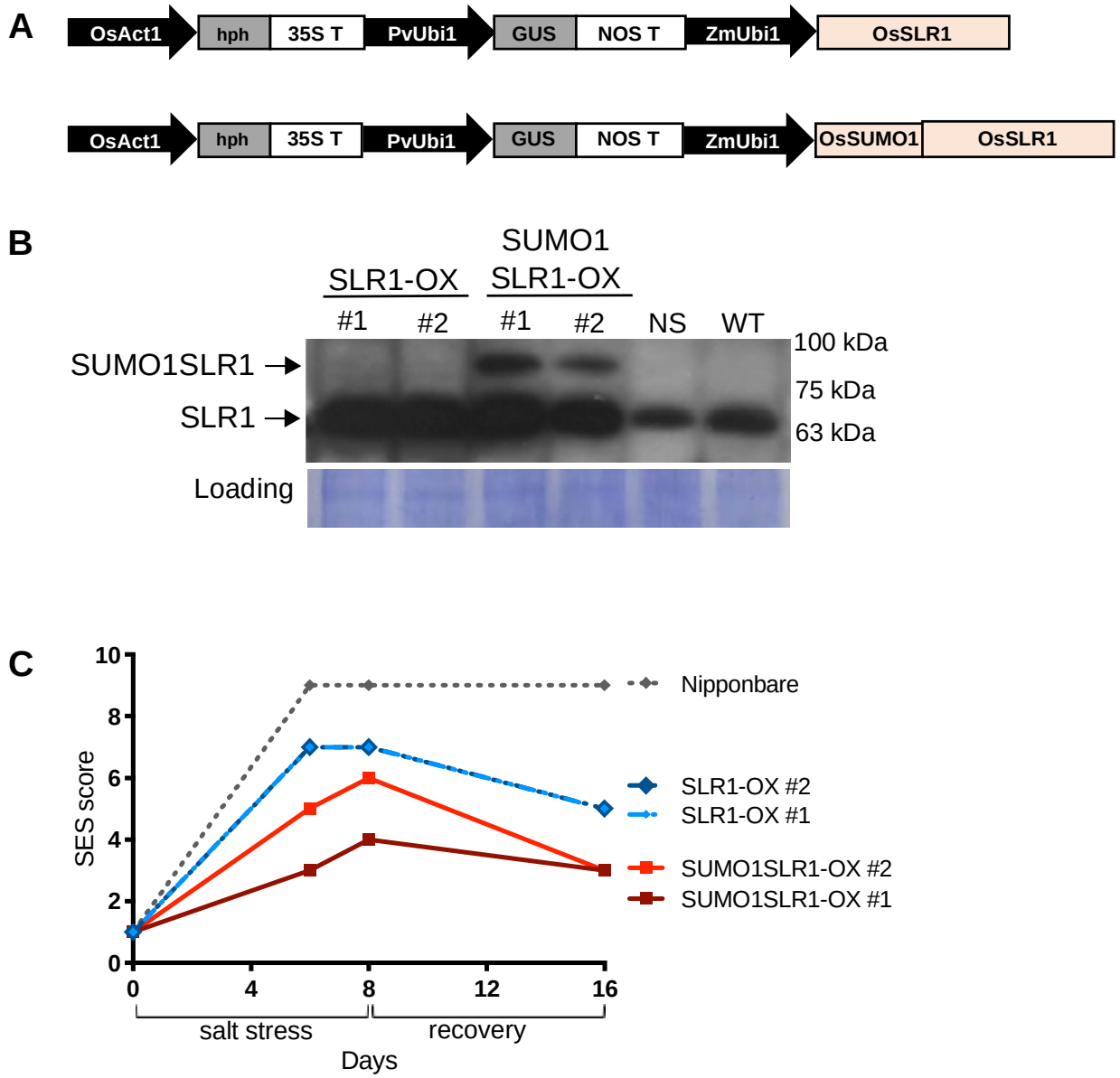

Figure 3. SLR1 SUMOylation confers salt tolerance at the seedling stage. (A) Depiction of gene constructs used to generate rice SLR1-OX and SUMO1SLR1-OX transgenic lines. *Zea mays* Ubi1 (ZmUbi1) promoter drives the expression of both OsSLR1 (SLR1-OX) and OsSLR1-OsSUMO1 gene fusion (SUMO1SLR1-OX). **(B)** SLR1 and SUMO1SLR1 protein accumulation in T2 independent transgenic lines (#1 and #2) of SUMO1SLR1-OX and SLR1-OX as detected by immunoblot using custom made anti-SLR1 antibody. **(C)** Stress severity as evaluated by IRRI salinity trial SES score for all lines in 6 and 8 days of stress and after 8 days of recovery period.

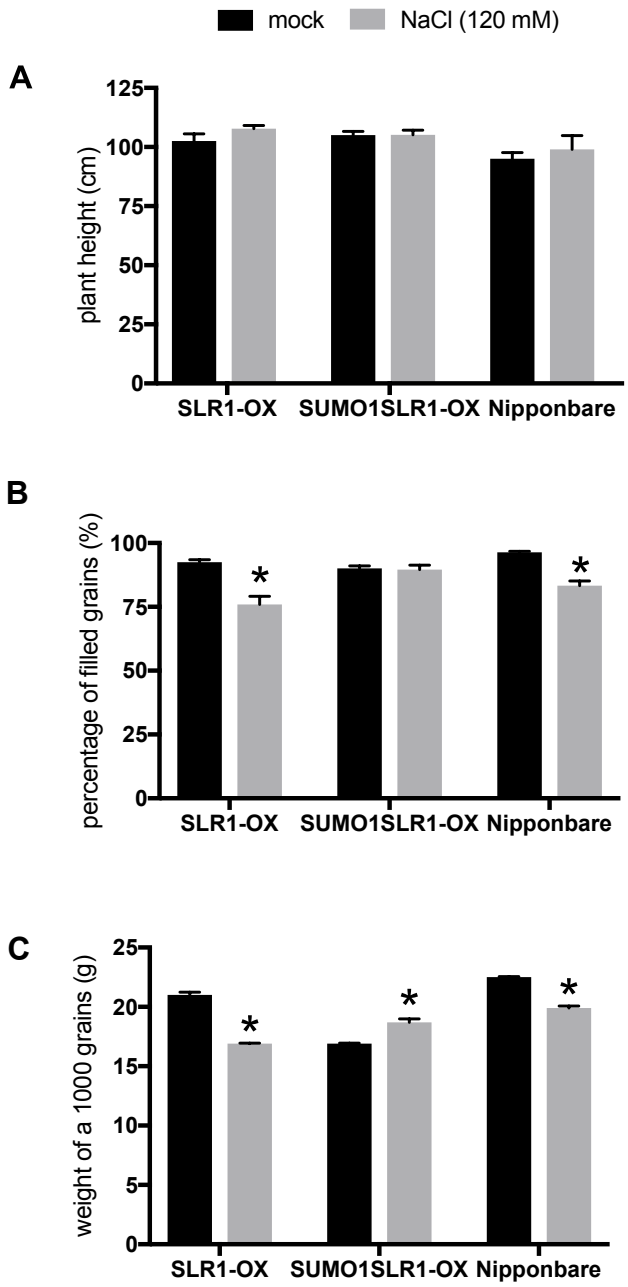

Figure 4. SLR1 SUMOylation reduces the impact of salt stress on yield. Agronomic parameters as measured at the end of rice life cycle: **(A)** plant height (N=6) **(B)** fertility as evaluated by the number of filled grains ratio to total panicle flowers (n>10) and **(C)** productivity as evaluated by the weight of 1000 grains (n>10). Error bars correspond to standard error (SE; 2 independent biological replicates with N=6 each) and statistically significant p-values represented as *($p<0.05$). The significance of statistics was asserted by t-test with Holm-Sidak method correction for multiple comparisons.

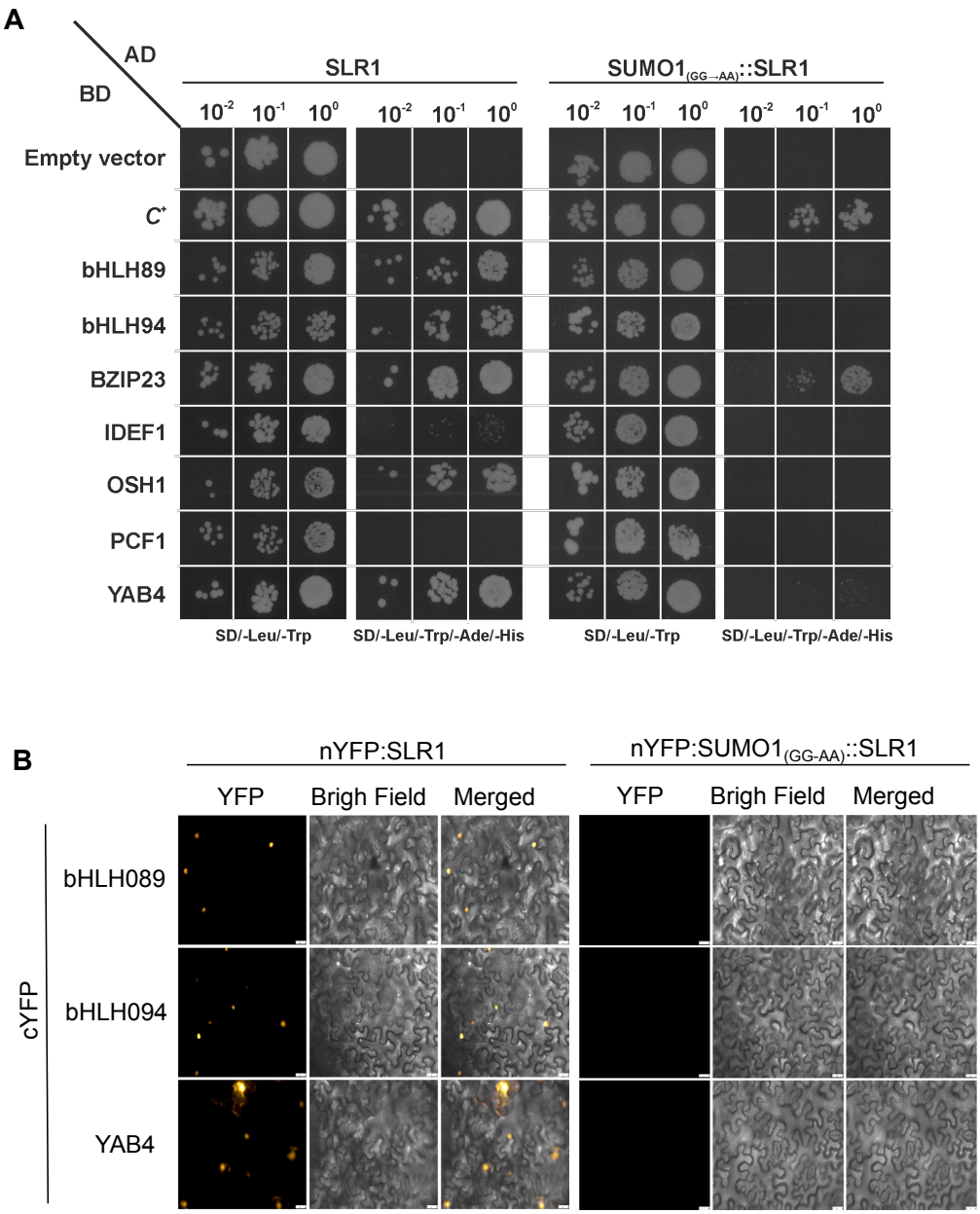

Figure 5. SLR1 SUMOylation affects its interaction with key transcription factors **(A)** Yeast-two hybrid (Y2H) analysis of both SLR1 and SUMO1SLR1. SUMO1::SLR1 fusion carries two mutations in the SUMO-protease cleavage motif (GG → AA) to avoid its removal by endogenous yeast proteases and guarantee constitutive SUMO attachment to SLR1 during the assay. Positive controls marked as (SD/-Leu/-Trip) and positive interactions marked with (SD/-Leu/-Trip/-Ade/-His). The vectors pAD-WT and pBD-WT (Stratagene) were used as positive control. **(B)** Bimolecular fluorescent complementation (BiFC) assays showing positive interactions between nYFP: SLR1 with cYFP:BHLH089, cYFP:BHLH094, and cYFP:YAB4. The presence of SUMO1 attached to lysine 2 of SLR1 (nYFP:SUMO1$_{(GG\text{-}AA)}$::SLR1) disrupts SLR1 interaction with these transcription factors. Negative controls for Y2H and BiFC assays can be found in Supplementary Figure S8.